Ocean Modelling 32 (2010) 36–43

Contents lists available at ScienceDirect

Ocean Modelling

journal homepage: www.elsevier.com/locate/ocemod

Global prediction of abyssal hill roughness statistics for use in ocean models from digital maps of paleo-spreading rate, paleo-ridge orientation, and sediment thickness

John A. Goff [a,*], Brian K. Arbic [b]

[a] Institute for Geophysics, Jackson School of Geosciences, University of Texas at Austin, JJ Pickle Research Campus, Bldg. 196, 10100 Burnet Rd. (R2200), Austin, TX 75758, USA
[b] Department of Oceanography and Center for Ocean-Atmospheric Prediction Studies, Florida State University P.O. Box 3064320 Tallahassee, FL 32306, USA

ARTICLE INFO

Article history:
Received 12 May 2009
Received in revised form 2 October 2009
Accepted 2 October 2009
Available online 8 October 2009

Keywords:
Abyssal hills
Roughness
Prediction
Ocean modeling

ABSTRACT

Abyssal hills are the dominant small-scale roughness fabric over much of the ocean floor. Created at mid-ocean ridges by combined volcanic and tectonic processes, they are rafted away by plate spreading and modified through time by mass wasting and sedimentation. Abyssal hills are morphological indicators of spreading rate and direction: they are lineated parallel to the ridge at the time of formation, and their heights and widths are inversely correlated to spreading rate. Knowledge of abyssal hill roughness statistics is important for high-resolution models, including models of internal wave generation and mixing driven by tidal and low-frequency flows over the rough bottom. In this paper we present a prediction of abyssal hill roughness statistical parameters world-wide via relationships for the average statistical properties of abyssal hills as a function of spreading rate and direction, and for the modification to these roughness parameters as a function of sediment thickness. These relationships are constrained by new publicly-available digital maps of paleo-spreading rate and direction, and sediment thickness. We also develop a new method for generating synthetic topography with variable statistical properties over a grid, and present an example of synthetic abyssal hill roughness generated for the North Atlantic on a 1/2-min grid.

1. Introduction

The small-scale roughness properties of the seafloor are increasingly being recognized as critical parameters in determining important processes in physical oceanography. For instance, in situ observations (e.g., Polzin et al., 1997) find that mixing levels are greatly elevated in regions of rough topography. Gille et al. (2000) demonstrate that mesoscale eddy energy tends to be lower in areas where the bottom is rough (suggesting the possibility that dissipation of eddy energy takes place in such areas), and Egbert and Ray (2003) show that substantial tidal dissipation occurs in such areas. The dissipation is generally thought to arise from the breaking of internal waves generated by flows over the rough seafloor. On the timescales of internal waves, mesoscale eddies and the general circulation can be regarded as steady, while tides are oscillatory. The detailed physics of linear internal wave generation is different for these two classes of motions (Bell, 1975), but for both types of flows the wave generation is strongly dependent on the horizontal and vertical scales inherent in the bottom topography. Using the classical formulation for lee waves (e.g., Cushman-Roisin, 1994), St. Laurent (1999) argued that horizontal scales ranging from 0.1 to 2.5 km generate internal waves when forced by steady flows. Features typical of abyssal hill morphology (e.g., 50 m height over 1 km horizontal scale) will generate a significant vertical internal wave energy flux. Carter et al. (2008) showed that high resolution of topography is also important for tides. They found that 0.01 degree (~1 km) resolution in an internal tide model results in 20% larger barotropic-to-baroclinic conversion than found in a model with 4-km resolution. Non-linear effects may be important as well, as some studies (e.g., Thurnherr and Richards, 2001; Thurnherr et al., 2002; Thurnherr and Speer, 2003; St. Laurent and Thurnherr, 2007) have argued from observational data that turbulence associated with hydraulic jumps occurs in areas of rough topography when the Froude number (Nh/U) exceeds an order one threshold. For typical values of the Brunt-Vaisala frequency (N) and of velocity (U) in the abyss (10^{-3} s^{-1} and 1 cm/s, respectively), this occurs when small-scale topography (h) exceeds about 10 m in height, which is typically the case for abyssal hill morphology.

A significant dilemma for physical oceanographers studying these processes (or, more generally, running ocean models at high horizontal resolution for any reason) is that the kind of bathymetric resolution required to model these processes over entire ocean basins are not available, nor will be any time soon. Acoustic

* Corresponding author. Tel.: +1 512 471 0476.
E-mail address: goff@ig.utexas (J.A. Goff).

1463-5003/$ - see front matter © 2009 Elsevier Ltd. All rights reserved.
doi:10.1016/j.ocemod.2009.10.001

bathymetric data, which can achieve lateral resolutions of 0.1–0.2 km, presently cover only a few percent of the ocean floor beyond the exclusive economic zones in coastal areas. A complete swath survey of all the deep oceans would take ~200 years of ship time at a cost of billions of dollars (Carron et al., 2001). The most comprehensive determination of bathymetry world-wide is the Smith and Sandwell (1994, 1997, 2004) model derived from satellite altimetry data combined with data from ship soundings. However, the resolution of this product is limited to >10 km in the deep ocean. Global bathymetry is also available from single-beam ship soundings, from which it is possible to obtain seafloor roughness properties to ~2 km scale (Becker and Sandwell, 2008). Coverage of these data is very sparse over much of the world's oceans, however. In addition, these data are not able to clearly establish abyssal hill orientations, or distinguish between abyssal hill morphology, which determines most of the small-scale component of bathymetry, and larger-scale features such as seamounts and fracture zones.

We seek to resolve this dilemma through a statistical modeling approach that globally predicts abyssal hill roughness properties based on paleo-spreading rates and directions, with modification by existing sediment cover. Abyssal hill statistical properties are modeled using the von Kármán statistical model (Goff and Jordan, 1988), which parameterizes rms heights, characteristic lengths and widths, strike orientation and fractal dimension. Predictions for unsedimented abyssal hill statistical properties are derived from a summary by Goff et al. (1997) of average von Kármán parameter values as a function of spreading rate, which were estimated from available near-ridge bathymetric data sets world-wide. Sediment modification is estimated using relationships developed by Webb and Jordan (2001) based on application of a diffusion model over rough surfaces. We present a global prediction of abyssal hill roughness parameters based on available maps of paleo-spreading properties (Müller et al., 2008) and sediment thickness (National Geophysical Data Center; http://www.ngdc.noaa.gov/mgg/sedthick/sedthick.html).

Numerical modeling of physical oceanographic processes, either at regional or global scales, requires adequate knowledge of the bathymetry at the model resolution scale. Although basin-wide or global determination of true bathymetry at abyssal hill scales is not feasible, we can create any number of synthetic realizations at arbitrary resolution that matches the statistical prediction. We propose that such realizations can be used as an overlay on the overly-smooth global bathymetric models (Smith and Sandwell, 1997, 2004) to provide realistic small-scale roughness texture for modeling purposes. A spectral method for generating synthetic topography from the von Kármán statistical model was introduced by Goff and Jordan (1988). However, spectral methods require homogeneity of statistical properties throughout the simulation grid, and so is unsuitable for these purposes because abyssal hill statistical properties will change significantly over the regional or global scales. We solve this problem by utilizing a spatial filter, whose characteristics vary with location, applied to an uncorrelated random field. Although computationally less efficient than the spectral method, this spatial filter method provides the flexibility required to simulate inhomogeneous fields.

2. Methods

2.1. Statistical modeling of abyssal hill morphology

Abyssal hills are generated at mid-ocean ridges by volcanic and tectonic processes (Macdonald et al., 1996), and modified through time by mass wasting (Goff and Tucholke, 1997) and sedimentation (Webb and Jordan, 2001). They tend to be highly lineated, with strike orientation parallel to the axis of the spreading ridge at the time of formation (Menard and Mammerickx, 1967). Abyssal hills are rough, exhibiting fractal behavior at scales smaller than ~2 to 10 km (Goff and Tucholke, 1997).

Goff and Jordan (1988) modeled the statistical behavior of abyssal hills using a von Kármán (1948) spectral model, adapted to two-dimensions and anisotropic in form to account for the linearity of the morphology. This model has a power-law (i.e., fractal) form at high wavenumbers, but is flat at low wavenumbers (which limits the variance), with the transition identified by an azimuthally-dependent corner wavenumber that defines a characteristic scale of the morphology. In two-dimensions, the abyssal hill spectral model is defined by:

$$P_h(\mathbf{k}) = \mathbf{4}\pi v \mathbf{H^2} |\mathbf{Q}|^{-\mathbf{1/2}} [\mathbf{u^2}(\mathbf{k}) + \mathbf{1}]^{-(\mathbf{v+1})}, \tag{1}$$

where H is the rms height, and v is the Hurst number, which determines the exponent of the power-law form at high wavenumbers. The function u is the dimensionless norm of the wavenumber vector $\mathbf{k}$ defined in terms of itsmodulus k and azimuth θ by

$$u(\mathbf{k}) = [\mathbf{k}^T Q^{-1} \mathbf{k}]^{1/2} = \sqrt{\left(\frac{k}{k_s}\right)^2 \cos^2(\theta - \theta_s) + \left(\frac{k}{k_n}\right)^2 \sin^2(\theta - \theta_s)} \tag{2}$$

The matrix $\mathbf{Q}$ is positive-definite and symmetric, expressed in terms of its ordered eigenvalues $k_n^2 \geqslant k_s^2$ and its normalized eigenvectors $\hat{\mathbf{e}}_n$ and $\hat{\mathbf{e}}_s$,

$$\mathbf{Q} = k_n^2 \hat{\mathbf{e}}_n \hat{\mathbf{e}}_n^T + k_s^2 \hat{\mathbf{e}}_s \hat{\mathbf{e}}_s^T. \tag{3}$$

Since the eigenvectors are orthogonal, they depend on only one orientation parameter, which we choose to be the azimuth θ_s of $\hat{\mathbf{e}}_s$, the eigenvector in the strike direction, measured clockwise from north. The fractal dimension is determined by the relationship $D = 3 - v$, and characteristic scales in the θ_s and θ_n directions are determined by (Goff and Jordan, 1988)

$$\lambda_n = \frac{2\sqrt{2(v+0.5)}}{k_n}; \quad \lambda_s = \frac{2\sqrt{2(v+0.5)}}{k_s}. \tag{4}$$

2.2. Dependence of abyssal hill statistics on spreading rate

Model parameters H^2, k_n, k_s, θ_s and v, which fully determine the von Kármán model, are estimated by a least-squares inversion of the covariance function empirically determined from gridded bathymetry data (Goff and Jordan, 1988). For reporting purposes, these parameters are typically translated into the more intuitive parameters H, λ_n, λ_s, θ_s and D. Regional studies of abyssal hill statistics for near-axis data were presented in Goff (1991), Goff et al. (1993, 1995, 1997), and Neumann and Forsyth (1995). These studies cover spreading rates ranging from ~24 to ~160 mm/yr (full rates), as well as a transition from axial-valley to axial-high types of spreading. The latter feature is an important component of the spreading rate dependency, as there is a significant step in both the rms heights and characteristic widths across the transition (Goff et al., 1997).

Goff et al. (1997) compiled average statistical values of H, λ_n, and λ_n/λ_s (abyssal hill aspect ratio) for all these regions, and plotted them as a function of spreading rate (Fig. 1). Abyssal hills tend to be taller, wider and less lineated at slower spreading ridges and, as noted above, there is a strong transition in rms heights and characteristic scales where the ridge axis changes from axial-valley to axial-high morphology. Heights and widths tend to correlate inversely with spreading rate over abyssal hills generated at axial-valley ridges, but are poorly correlated to spreading rates over abyssal hills generated at axial-high ridges. Locally, values of H reported by these studies can vary by ±20–30% rms relative to the averages,

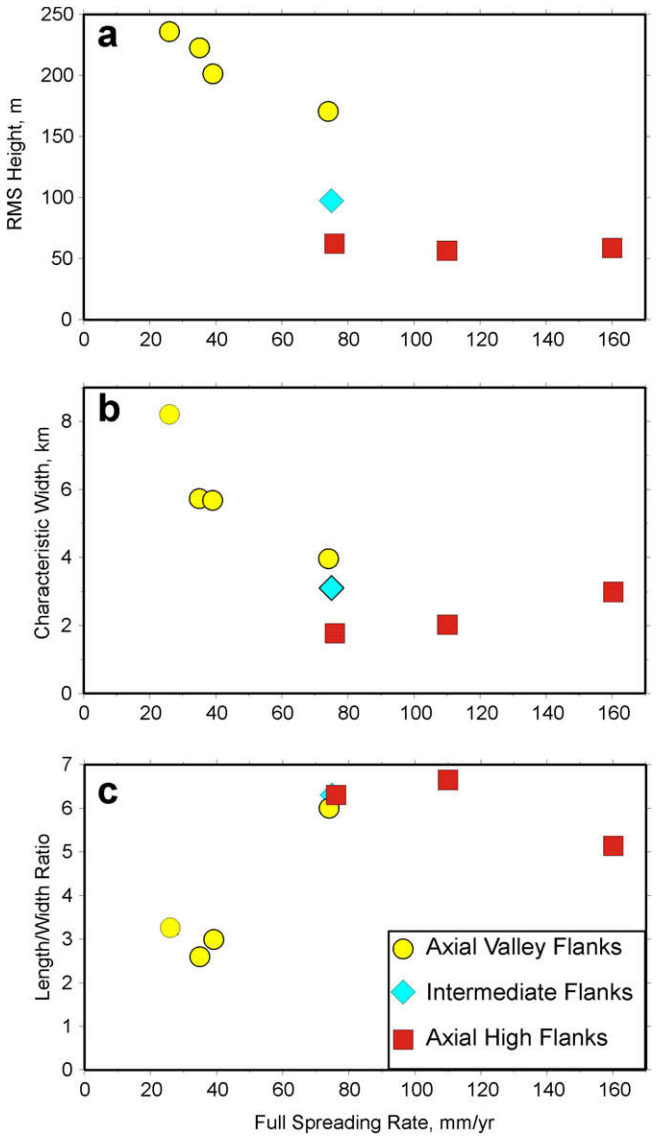

Fig. 1. Regional mean values for abyssal hill (a) rms height (H), (b) characteristic width λ_n, and (c) the ratio of characteristic length/characteristic width (λ_n/λ_s), plotted as a function of full spreading rate (replotted from Goff et al., 1997. Interpolation/extrapolation of these values is used to predict the relationship between paleo-spreading rates and unsedimented abyssal hill roughness statistical parameters.

and λ_n and λ_s, by ±30–50% rms. Ridge segmentation and crustal thickness are secondary factors that influence abyssal hill morphology (for example, abyssal hills tend to be shorter and thinner where crustal thickness is greater and/or further removed from a segment boundary). Fractal dimensions, often difficult to estimate with reliability, were not found to vary with spreading rate, typically having values of ~2.2 to 2.3 for unsedimented seafloor (Goff, 1991).

The empirical relationship between spreading rate and abyssal hill morphology presented in Fig. 1 forms the basis for our prediction of abyssal hill roughness parameters throughout the ocean basins. For this initial effort, we will neglect secondary effects such as segmentation or crustal thickness, both because such relationships are not as readily quantifiable, and because such constraints are not readily available over the whole ocean basin. We will address this issue further in discussing the results. Interpolating/extrapolating linearly among the average values in Fig. 1, we can establish the predicted rms height (H), and characteristic width (λ_n) and length (λ_s) for unsedimented seafloor given knowledge of the paleo-spreading rate at the time of formation. The fractal dimension (D) is assumed to be 2.2 ($\nu = 0.8$; values of k_n and k_s are determined via the inverse to Eq. (3)). Finally, abyssal hill lineaments (θ_s) can be predicted from paleo-ridge azimuths (the direction normal to paleo-spreading directions). Recent global maps of paleo-spreading rate (Fig. 2) and paleo-ridge azimuths (Fig. 3) are available from Müller et al. (2008).

2.3. Modifications to abyssal hill roughness by sediment drape

Sediment drape is a major modifier to abyssal hill morphology (Bird and Pockalny, 1994), and can completely obscure abyssal hill morphology when sediment thickness is greater than about twice the rms height (Webb and Jordan, 2001). Our global predictions of abyssal hill roughness must be modified by available information about the sediment cover. A global compilation of sediment thickness is available from the National Geophysical Data Center (Fig. 4; http://www.ngdc.noaa.gov/mgg/sedthick/sedthick.html).

Webb and Jordan (2001) investigated the quantitative effects of sediment drape on basement morphology by applying a numerical model of pelagic sedimentation. Their algorithm modeled the ensemble result of post-depositional sediment transport as a diffusive process in which the downhill flux of material is proportional to the seafloor slope via a variable diffusivity parameter. Running forward models at realistic diffusivity over a range of two-dimensional synthetic surfaces corresponding to the von Kármán model, Webb and Jordan (2001) established an empirical relationship for the functionality of rms height (H) as a function of the total sediment thickness (S):

$$H(S) = H_0 - S/2, \quad \text{for} \quad S/2 < H_0,$$
$$H(S) = 0, \quad \text{for} \quad S/2 \geqslant H_0 \tag{5}$$

where $H_0 = H(0)$ is the unsedimented abyssal hill rms height, which we predict by the spreading rate relationship expressed in Fig. 1. Webb and Jordan (2001) likewise determined an empirical relationship between characteristic width (λ_n) and sediment thickness, but expressed in terms of the ratio between sediment thickness and rms height:

$$\lambda_n(S/H_0) = \lambda_{n,0} + 1.3\lambda_{n,0}S/H_0, \tag{6}$$

where $\lambda_{n,0} = \lambda_n(0)$ is the unsedimented characteristics width, which we also predict from Fig. 1. Webb and Jordan (2001) did not explicitly investigate the effect of sediment drape on characteristic length, but there is no reason to assume any different relationship than expressed for characteristic width. Hence, for our purposes we assume:

$$\lambda_s(S/H_0) = \lambda_{s,0} + 1.3\lambda_{s,0}S/H_0. \tag{7}$$

Webb and Jordan (2001) also investigated the effect of pelagic sediment drape on the fractal dimension (their Fig. 10d). Not surprisingly, such drape decreases the fractal dimension rapidly with increasing sediment thickness, as small-scale undulations are preferentially filled in. Webb and Jordan (2001) did not, however, suggest an empirical relationship for fractal dimension as a function of sediment cover. Nevertheless, using their Fig. 10d, and assuming $D = 2.2$ for unsedimented seafloor (Goff et al., 1997), we estimate the following:

$$D(S/H_0) = 2.2 - 1.5(S/H_0), \quad \text{for} \quad S/H_0 \leqslant 0.1$$
$$D(S/H_0) = 2.05, \quad \text{for} \quad S/H_0 > 0.1. \tag{8}$$

The relationships expressed in Eqs. (5)–(8), combined with available information on global sediment thickness (Fig. 4), provide modifications to our predictions of abyssal hill roughness based on paleo-spreading rates.

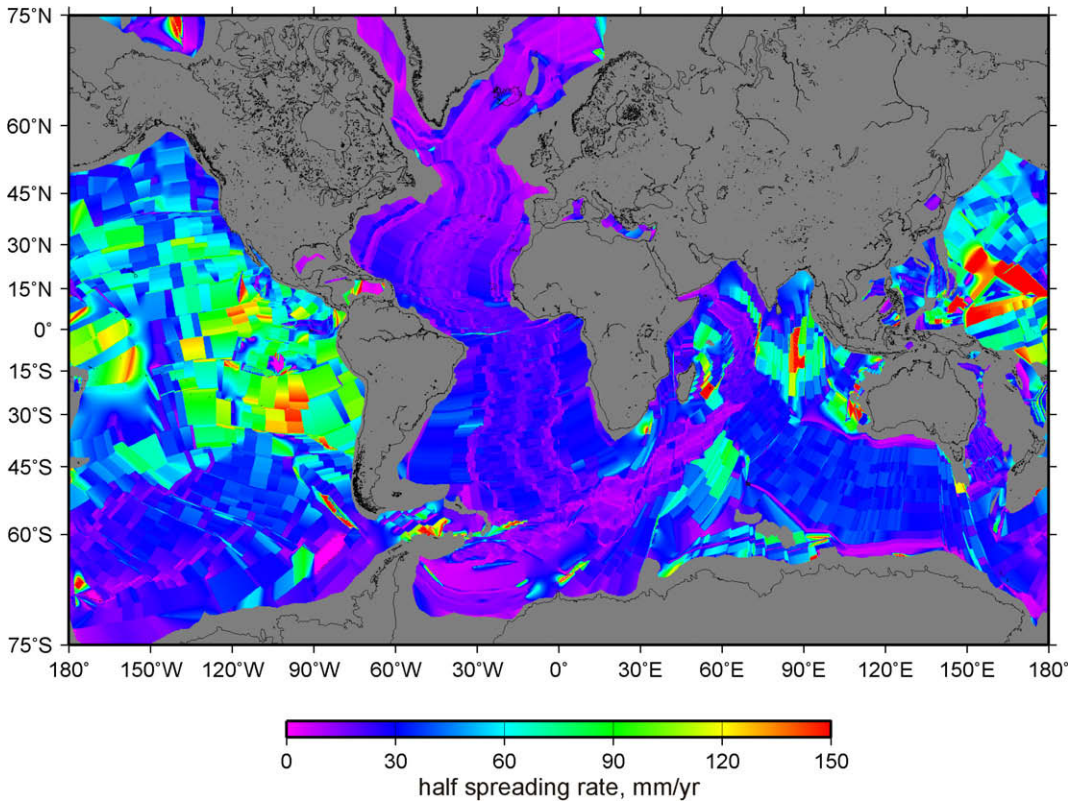

Fig. 2. Global paleo-half spreading rates. Data from Müller et al. (2008).

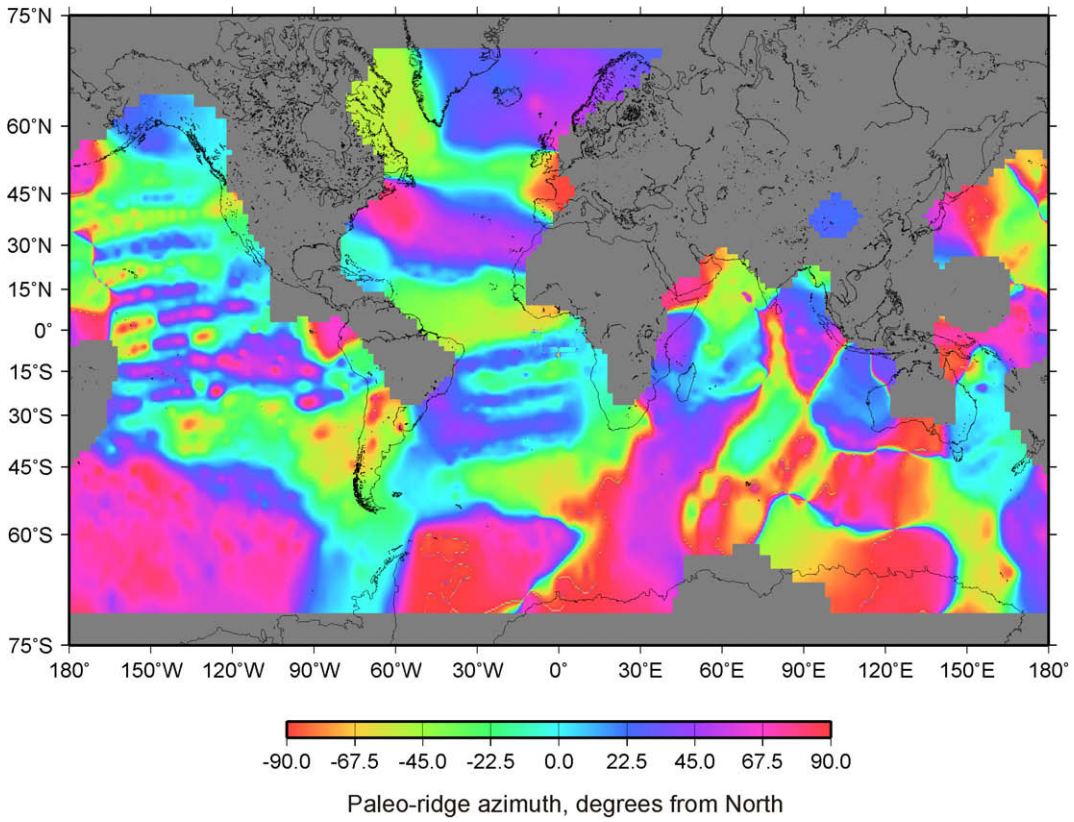

Fig. 3. Global paleo-ridge azimuths. Data from Müller et al. (2008).

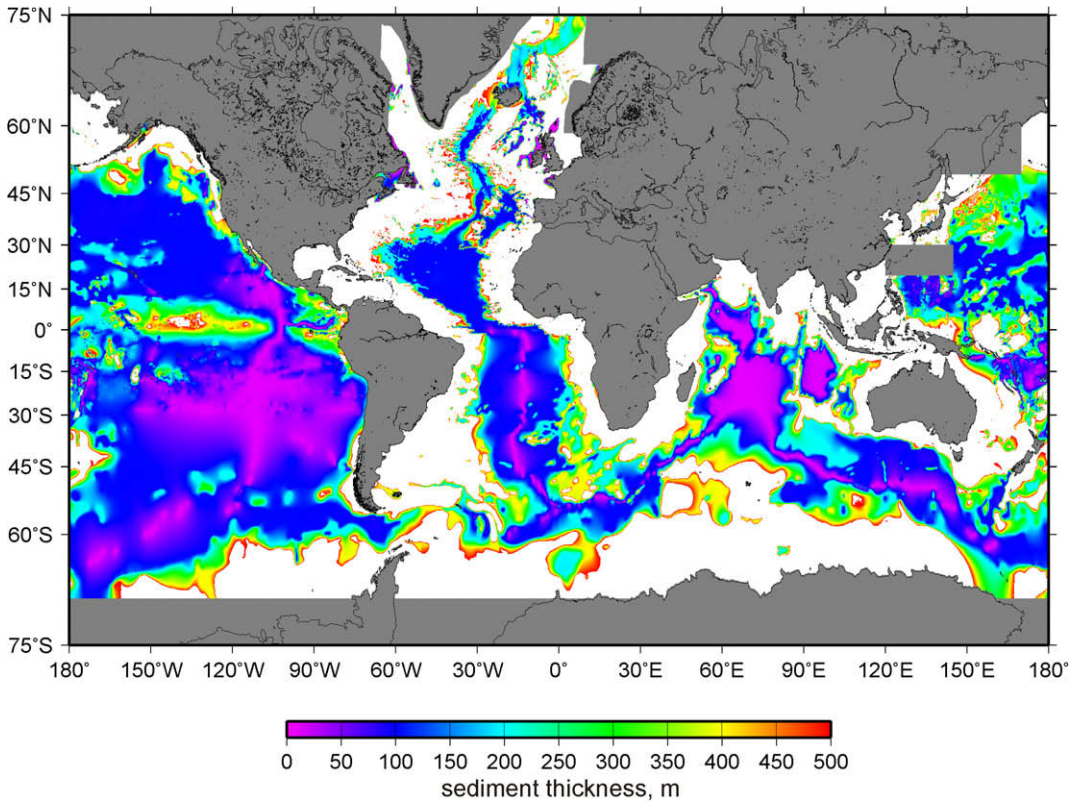

Fig. 4. Sediment thickness over the Earth's ocean basins (regions with >500 m thickness are colored white). Data from the National Geophysical Data Center (http://www.ngdc.noaa.gov/mgg/sedthick/sedthick.html).

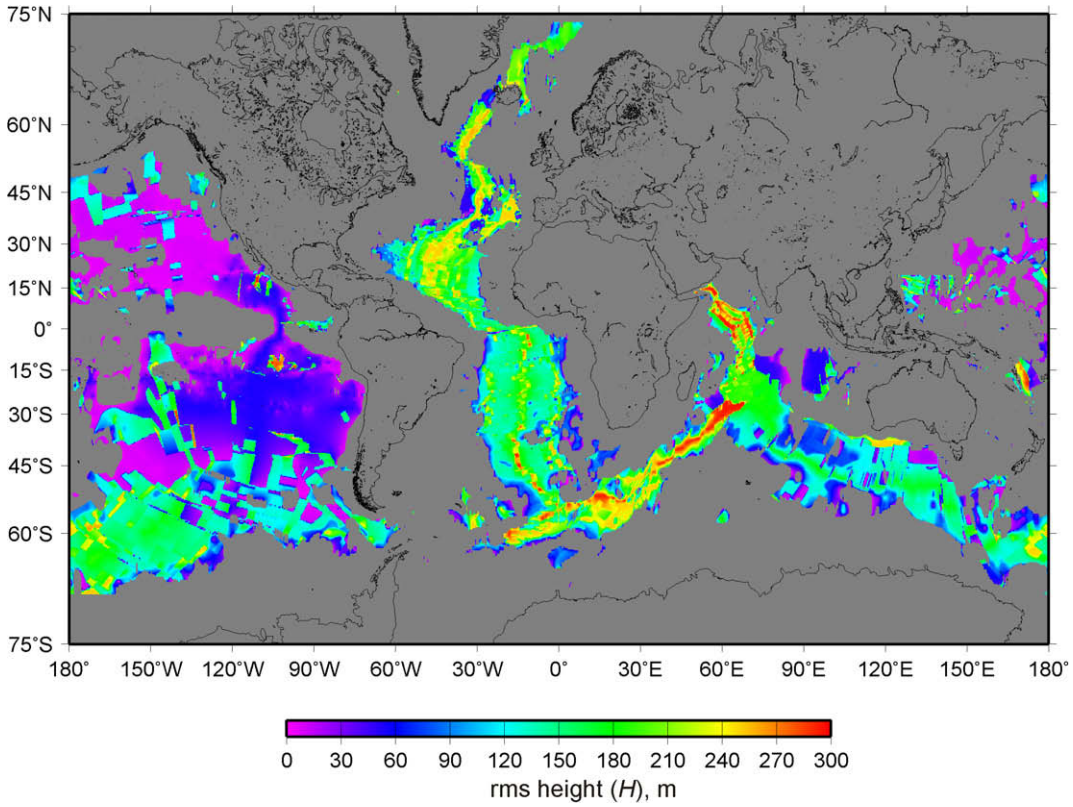

Fig. 5. Global predicted abyssal hill rms heights. Gray areas indicate regions of no predicted abyssal hill roughness due to sediment cover.

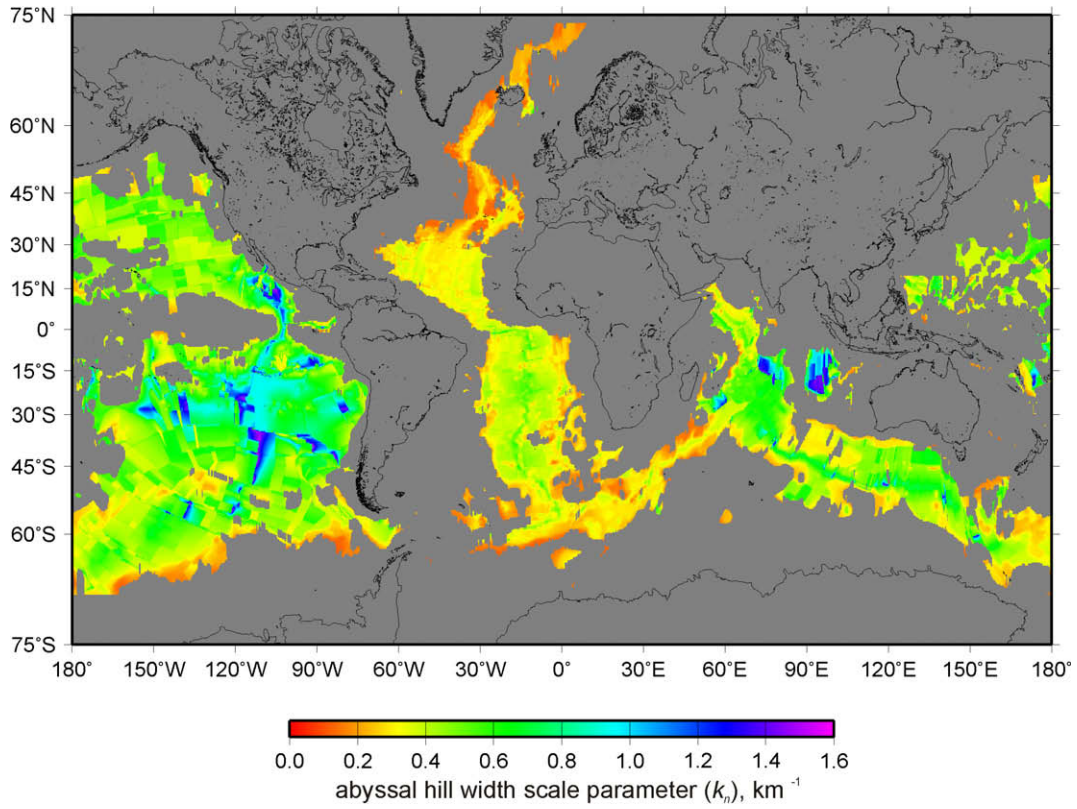

Fig. 6. Global predicted abyssal hill width scale parameter. Gray areas indicate regions of no predicted abyssal hill roughness due to sediment cover.

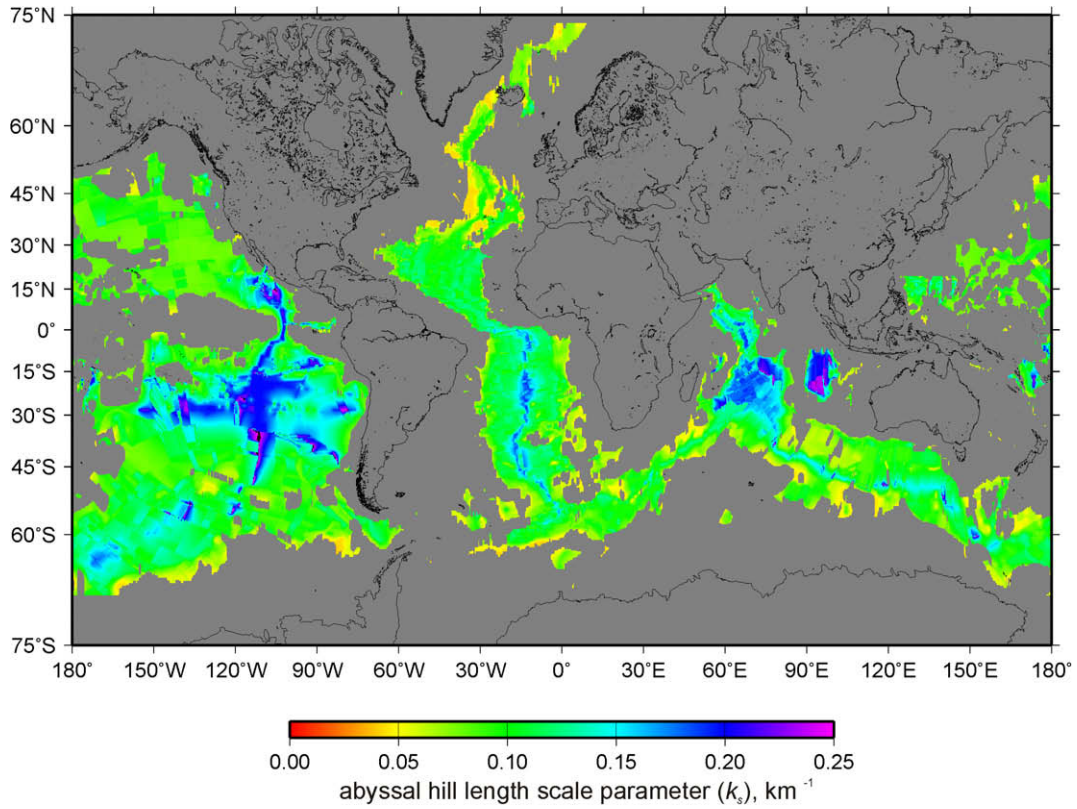

Fig. 7. Global predicted abyssal hill length scale parameter. Gray areas indicate regions of no predicted abyssal hill roughness due to sediment cover.

3. Results and discussion

Global predictions are shown for abyssal hill rms heights, H (Fig. 5), the width scale parameter k_n (Fig. 6), and the length scale parameter, k_s (Fig. 7), at a resolution of 0.25° latitude by 0.25° longitude. Gray areas in these maps are regions where abyssal hills are completely masked by sediment cover, which appears to be well over half the global ocean basins. Abyssal hill orientations are identical to Fig. 3. Fractal dimensions in the prediction (not shown) are 2.05 everywhere but in a narrow zone about the ridge axes, due to the rapid reduction in fractal dimension dictated by Eq. (8).

These maps thus represent our prediction of the abyssal hill component of seafloor roughness parameters based on available knowledge of paleo-spreading rates and directions, and total sediment cover. These results do not predict additional roughness associated with larger-scale features such as spreading ridges, fracture zones, or seamounts. However, roughness on these larger scales does not require prediction, as such features are generally well-characterized in the altimetry-derived bathymetry maps (Smith and Sandwell, 2004).

As noted above, abyssal hill roughness is correlated to more than just spreading rate (e.g., crustal thickness, proximity to segment boundaries), and thus these maps must be considered as first-order predictions subject to refinement in the future. These maps fail to predict, for example, the enhanced abyssal hill roughness within the Australian Antarctic Discordance, south of Australia, which has thinner-than-normal oceanic crust (West et al., 1994; Christie et al., 1998), or the reduced roughness on the flanks of the slow-spreading Reykjanes Ridge, part of the Mid Atlantic Ridge south of Iceland, which has thicker-than-normal oceanic crust (Searle et al., 1998). A more sophisticated prediction would be possible if both crystalline oceanic crustal thickness could be resolved over the ocean basins and a quantitative relationship between crustal thickness and abyssal hill morphology (a secondary effect to spreading rate) could be derived.

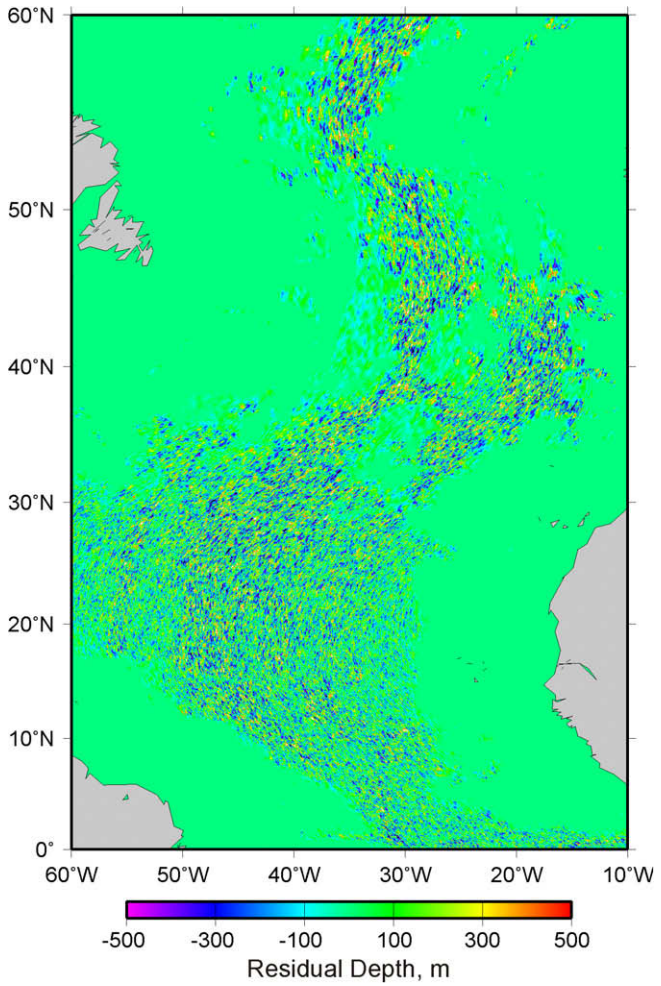

Fig. 8. Synthetic realization of abyssal hill topography in the North Atlantic Ocean based on predicted statistical parameters.

4. Synthetic abyssal hill roughness

Because abyssal hills dominate topographic variance at small scales, synthetic abyssal hill roughness is desirable for use in high-resolution global or regional numerical models of tides and the oceanic general circulation. We anticipate in particular that synthetic abyssal hill topography can be used as an overlay on existing, lower-resolution maps of seafloor bathymetry (e.g., Smith and Sandwell, 2004) in order to produce a seafloor map that, in a statistical sense, exhibits realistic roughness properties at small scales.

Spectral methods are the most efficient means of generating synthetic topography from a 2nd-order statistical model. To do so for the von Kármán model (Goff and Jordan, 1989), we first compute a Fourier spectrum on a regularly-spaced wavenumber grid by multiplying the amplitude spectrum, defined as the square root of the power spectrum (Eq. (1)), by a phase factor $\exp(i\varphi)$, where φ is a random number uniformly distributed on the interval $(0, 2\pi)$. After enforcing Hermetian symmetry, the space-domain image is then obtained from a two-dimensional, fast Fourier transform. The uniformly distributed random phase ensures that the image is normally distributed (Priestly, 1981).

The spectral method has a critical drawback, however: it can only be used to generate statistically homogeneous fields (i.e., the statistical properties do not vary by location). The spectral method is not, therefore, suitable for generating a global abyssal hill realization because the statistical properties are highly inhomogeneous. An alternative to the spectral method of simulation is to perform the equivalent operation in the space domain: convolution of the filter (the inverse Fourier transform of the amplitude spectrum) with a Gaussian-distributed, uncorrelated random noise field of unit variance (the Fourier transform of the phase spectrum). In our algorithm, the functional form of the filter changes with location to correspond to the predicted statistical parameters (Figs. 5–7). Although computationally far more intensive, modern computing power renders the solution tractable on a global scale. We have been able to generate global realizations on grid with a 1/2 by 1/2-min node spacing, using a filter range of 65 by 65 node points, in less than a day of computing time on a 2-processor, SunFire 4200 workstation. The node spacing was chosen to correspond to anticipated global oceanographic modeling requirements; in principal this value can be chosen to be arbitrarily small.

A section of our realization, from the North Atlantic Ocean, is presented in Fig. 8. Depths are presented here as a residual, intended for overlay on a low-resolution bathymetry map. The inhomogeneity of the realization is evident, with spatial variations in the amplitudes, widths and orientations of the abyssal hills. The older parts of the basin, near the continental margins, are sufficiently covered by sediment that no abyssal hill roughness is predicted.

5. Conclusions

The inability of global bathymetric relief maps to resolve roughness at scales less than ~10 km is a significant potential detriment

to future efforts to model the generation of internal waves by the low-frequency and tidal flows over rough topography. More generally, as increasing computer power allows for ocean models with higher and higher horizontal resolution, it becomes a matter of concern that the resolution of available global bathymetric datasets does not match the model resolutions. The methodology presented here aims to address that deficiency by providing a prediction of the statistical characteristics, using the von Kármán parameterized model, of abyssal hill roughness world-wide. The method is based on two relationships: (1) an empirical relationship between mid-ocean ridge spreading rates and average von Kármán parameters estimated from flanking abyssal hills, and (2) a numerical model-derived relationship between pelagic sediment thickness and consequent modification to the statistical characteristics. This is a first-order prediction that does not take into account secondary influences on abyssal hill roughness, such as regional variations in crustal thickness, or proximity to segment discontinuities. Insufficient information is available at this time to constrain such factors. The prediction of statistical properties can also be used to generate synthetic realizations of abyssal hill roughness world-wide. Applied as an overlay to lower-resolution bathymetric maps, these realizations can be used to provide realistic small-scale roughness for global or basin-wide numerical models of ocean circulation.

Acknowledgements

The authors gratefully acknowledge the support of the Office of Naval Research under Grant N00014-07-1-0392. We appreciate constructive discussions with Walter Smith and David Sandwell. This is UTIG contribution #2139.

References

Becker, J.J., Sandwell, D.T., 2008. Global estimates of seafloor slope from single-beam ship soundings. J. Geophys. Res. 113, C05028. doi:10.1029/2006JC003879.

Bell, T.H., 1975. Lee waves in stratified flows with simple harmonic time dependence. J. Fluid Mech. 67, 705–722.

Bird, R.T., Pockalny, R.A., 1994. Late Cretaceous and Cenozoic seafloor and oceanic basement roughness: Spreading rate, crustal age and sediment thickness corrections. Earth Planet. Sci. Lett. 123, 239–254.

Carron, M.J., Vogt, P.R., Jung, W.-Y., 2001. A proposed international long-term project to systematically map the world's ocean floors from beach to trench: GOMaP (Global Ocean Mapping Program). Int. Hydrogr. Rev. 2, 49–55.

Carter, G.S., Merrifield, M.A., Luther, D.S., Becker, J.M., Katsumata, K., Gregg, M.C., Levine, M.D., Boyd, T.J., Firing, Y.L., 2008. Energetics of M_2 barotropic-to-baroclinic tidal conversion at the Hawaiian Islands. J. Physi. Oceanogr. 38, 2205–2223.

Christie, D.M., West, B.P., Pyle, D.G., Hanan, B.B., 1998. Chaotic topography, mantle flow and mantle migration in the Australian–Antarctic discordance. Nature 394, 637–644.

Cushman-Roisin, B., 1994. Introduction to geophysical fluid dynamics. Prentice-Hall, Englewood Cliffs. 320 pp.

Egbert, G.D., Ray, R.D., 2003. Semi-diurnal and diurnal tidal dissipation from TOPEX/Poseidon altimetry. Geophys. Res. Lett. 30, 1907. doi:10.1029/2003GL017676.

Gille, S.T., Yale, M.M., Sandwell, D.T., 2000. Global correlation of mesoscale ocean variability with seafloor roughness from satellite altimetry. Geophys. Res. Lett. 27, 1251–1254.

Goff, J.A., 1991. A global and regional stochastic analysis of near-ridge abyssal hill morphology. J. Geophys. Res. 96, 21713–21737.

Goff, J.A., Jordan, T.H., 1988. Stochastic modeling of seafloor morphology: inversion of sea beam data for second-order statistics. J. Geophys. Res. 93, 13589–13608.

Goff, J.A., Jordan, T.H., 1989. Stochastic modeling of seafloor morphology: a parameterized Gaussian model. Geophys. Res. Lett. 16, 45–48.

Goff, J.A., Tucholke, B.E., 1997. Multi-scale spectral analysis of bathymetry on the flank of the Mid-Atlantic Ridge: Modification of the seafloor by mass wasting and sedimentation. J. Geophys. Res. 102, 15447–15462.

Goff, J.A., Malinverno, A., Fornari, D.J., Cochran, J.R., 1993. Abyssal hill segmentation: quantitative analysis of the East Pacific Rise flanks 7°S–9°S. J. Geophys. Res. 98, 13851–13862.

Goff, J.A., Tucholke, B.E., Lin, J., Jaroslow, G.E., Kleinrock, M.C., 1995. Quantitative analysis of abyssal hills in the Atlantic Ocean: A correlation between inferred crustal thickness and extensional faulting. J. Geophys. Res. 100, 22509–22522.

Goff, J.A., Ma, Y., Shah, A., Cochran, J.R., Sempéré, J.-C., 1997. Stochastic analysis of seafloor morphology on the flank of the Southeast Indian Ridge: the influence of ridge morphology on the formation of abyssal hills. J. Geophys. Res. 102, 15521–15534.

Macdonald, K.C., Fox, P.J., Alexander, R.T., Pockalny, R., Gente, P., 1996. Volcanic growth faults and the origin of Pacific abyssal hills. Nature 380, 125–129.

Menard, H.W., Mammerickx, J., 1967. 1967. Abyssal hills, magnetic anomalies and the East Pacific Rise. Earth Planet. Sci. Lett. 2, 465–472.

Müller, R.D., Sdrolias, M., Gaina, C., Roest, W.R., 2008. Age, spreading rates and spreading symmetry of the world's ocean crust. Geochem. Geophys. Geosyst. 9, Q04006. doi:10.1029/2007GC001743.

Neumann, G.A., Forsyth, D.W., 1995. High resolution statistical estimation of seafloor morphology: Oblique and orthogonal fabric on the flanks of the Mid-Atlantic Ridge, 34–35.5 S. Mar. Geophys. Res. 17, 221–250.

Polzin, K.L., Toole, J.M., Ledwell, J.R., Schmitt, R.W., 1997. Spatial variability of turbulent mixing in the abyssal ocean. Science 276, 93–96.

Priestly, M.B., 1981. Spectral Analysis and Time Series. Academic Press, London. 890 pp.

St. Laurent, L.C., 1999. Diapycnal advection by double diffusion and turbulence in the ocean. Doctoral Dissertation, MIT/WHOI Joint Program, MIT/WHOI 99-12, Cambridge and Woods Hole, MA, 139 pp.

St. Laurent, L.C., Thurnherr, A.M., 2007. Intense mixing of lower thermocline water on the crest of the Mid-Atlantic Ridge. Nature 448. doi:10.1038/nature06043.

Searle, R.C., Keeton, J.A., Owens, R.B., White, R.S., Mecklenburg, R., Parsons, B., Lee, S.M., 1998. The Reykjanes Ridge: structure and tectonics of a hot-spot-influenced slow-spreading ridge, from multibeam bathymetry, gravity and magnetic investigations. Earth Planet. Sci. Lett. 160, 463–478.

Smith, W.H.F., Sandwell, D.T., 1994. Bathymetric prediction from dense satellite altimetry and sparse shipboard bathymetry. J. Geophys. Res. 99, 21803–21824.

Smith, W.H.F., Sandwell, D.T., 1997. Global seafloor topography from satellite altimetry and ship depth soundings: evidence for stochastic reheating of the oceanic lithosphere. Science 277, 1956–1962.

Smith, W.H.F., Sandwell, D.T., 2004. Conventional bathymetry, bathymetry from space, and geodetic altimetry. Oceanography 17, 8–23.

Thurnherr, A.M., Richards, K.J., 2001. Hydrography and high-temperature heat flux of the Rainbow hydrothermal site (36 14′N, Mid-Atlantic Ridge). J. Geophys. Res. 106, 9411–9426.

Thurnherr, A.M., Speer, K.G., 2003. Boundary mixing and topographic blocking on the Mid-Atlantic Ridge in the South Atlantic. J. Phys. Oceanogr. 33, 848–862.

Thurnherr, A.M., Richards, K.J., German, C.R., Lane-Serff, G.F., Speer, K.G., 2002. Flow and mixing in the rift valley of the Mid-Atlantic Ridge. J. Phys. Oceanogr. 32, 1763–1778.

von Kármán, T., 1948. Progress in the statistical theory of turbulence. Proceedings of the National Academy of Science 34, 530–539.

Webb, H.F., Jordan, T.H., 2001. Pelagic sedimentation on rough seafloor topography 1. Forward model. J. Geophys. Res. 106, 30433–30449.

West, B.P., Sempéré, J.-C., Pyle, D.G., Phipps Morgan, J., Christie, D.M., 1994. Evidence for variable upper mantle temperature and crustal thickness in and near the Australian–Antarctic discordance. Earth Planet. Sci. Lett. 128, 135–153.